

Search for CP violation with kinematic asymmetries in the $D^0 \rightarrow K^+ K^- \pi^+ \pi^-$ decay

J. B. Kim,³⁸ E. Won,^{38,*} I. Adachi,^{17,13} H. Aihara,⁸⁵ S. Al Said,^{79,35} D. M. Asner,³ H. Atmacan,⁷⁵ V. Aulchenko,^{4,64} T. Aushev,⁵⁴ V. Babu,⁸⁰ I. Badhrees,^{79,34} S. Bahinipati,²¹ A. M. Bakich,⁷⁸ V. Bansal,⁶⁶ P. Behera,²⁴ C. Beleño,¹² B. Bhuyan,²² T. Bilka,⁵ J. Biswal,³¹ A. Bobrov,^{4,64} A. Bozek,⁶² M. Bračko,^{48,31} L. Cao,³² D. Červenkov,⁵ P. Chang,⁶¹ V. Chekelian,⁴⁹ A. Chen,⁵⁹ B. G. Cheon,¹⁵ K. Chilikin,⁴² K. Cho,³⁷ S.-K. Choi,¹⁴ Y. Choi,⁷⁷ D. Cinabro,⁸⁹ S. Cunliffe,⁷ N. Dash,²¹ S. Di Carlo,⁴⁰ Z. Doležal,⁵ T. V. Dong,^{17,13} S. Eidelman,^{4,64,42} D. Epifanov,^{4,64} J. E. Fast,⁶⁶ T. Ferber,⁷ A. Frey,¹² B. G. Fulsom,⁶⁶ R. Garg,⁶⁷ V. Gaur,⁸⁸ N. Gabyshev,^{4,64} A. Garmash,^{4,64} M. Gelb,³² A. Giri,²³ P. Goldenzweig,³² D. Greenwald,⁸¹ Y. Guan,^{25,17} J. Haba,^{17,13} T. Hara,^{17,13} K. Hayasaka,⁶³ H. Hayashii,⁵⁸ W.-S. Hou,⁶¹ T. Iijima,^{56,55} K. Inami,⁵⁵ G. Inguglia,⁷ A. Ishikawa,⁸³ R. Itoh,^{17,13} M. Iwasaki,⁶⁵ Y. Iwasaki,¹⁷ S. Jia,² Y. Jin,⁸⁵ D. Joffe,³³ G. Karyan,⁷ T. Kawasaki,³⁶ H. Kichimi,¹⁷ C. Kiesling,⁴⁹ D. Y. Kim,⁷⁴ H. J. Kim,³⁹ S. H. Kim,¹⁵ K. Kinoshita,⁶ P. Kodyš,⁵ S. Korpar,^{48,31} D. Kotchetkov,¹⁶ P. Križan,^{43,31} R. Kroeger,⁵¹ P. Krokovny,^{4,64} R. Kulasiri,³³ A. Kuzmin,^{4,64} Y.-J. Kwon,⁹¹ Y.-T. Lai,¹⁷ K. Lalwani,⁴⁶ J. S. Lange,¹⁰ I. S. Lee,¹⁵ J. K. Lee,⁷² J. Y. Lee,⁷² S. C. Lee,³⁹ C. H. Li,⁵⁰ L. K. Li,²⁶ Y. B. Li,⁶⁸ L. Li Gioi,⁴⁹ J. Libby,²⁴ Z. Liptak,¹⁶ D. Liventsev,^{88,17} P.-C. Lu,⁶¹ M. Lubej,³¹ T. Luo,⁹ J. MacNaughton,⁵² M. Masuda,⁸⁴ T. Matsuda,⁵² D. Matvienko,^{4,64,42} M. Merola,^{28,57} K. Miyabayashi,⁵⁸ R. Mizuk,^{42,53,54} G. B. Mohanty,⁸⁰ H. K. Moon,³⁸ T. Mori,⁵⁵ M. Mrvar,³¹ R. Mussa,²⁹ E. Nakano,⁶⁵ M. Nakao,^{17,13} K. J. Nath,²² M. Nayak,^{89,17} N. K. Nisar,⁶⁹ S. Nishida,^{17,13} S. Ogawa,⁸² G. Pakhlova,^{42,54} B. Pal,³ S. Pardi,²⁸ H. Park,³⁹ S. Paul,⁸¹ T. K. Pedlar,⁴⁵ R. Pestotnik,³¹ L. E. Piilonen,⁸⁸ V. Popov,^{42,54} K. Prasanth,⁸⁰ E. Prencipe,¹⁹ A. Rabusov,⁸¹ P. K. Resmi,²⁴ M. Ritter,⁴⁴ A. Rostomyan,⁷ G. Russo,²⁸ Y. Sakai,^{17,13} M. Salehi,^{47,44} S. Sandilya,⁶ L. Santelj,¹⁷ T. Sanuki,⁸³ V. Savinov,⁶⁹ O. Schneider,⁴¹ G. Schnell,^{1,20} C. Schwanda,²⁷ Y. Seino,⁶³ K. Senyo,⁹⁰ O. Seon,⁵⁵ C. P. Shen,² T.-A. Shibata,⁸⁶ J.-G. Shiu,⁶¹ E. Solovieva,^{42,54} M. Starič,³¹ J. F. Strube,⁶⁶ M. Sumihama,¹¹ T. Sumiyoshi,⁸⁷ W. Sutcliffe,³² M. Takizawa,^{73,18,70} K. Tanida,³⁰ Y. Tao,⁸ F. Tenchini,⁷ M. Uchida,⁸⁶ T. Uglov,^{42,54} Y. Unno,¹⁵ S. Uno,^{17,13} P. Urquijo,⁵⁰ R. Van Tonder,³² G. Varner,¹⁶ B. Wang,⁶ C. H. Wang,⁶⁰ M.-Z. Wang,⁶¹ P. Wang,²⁶ X. L. Wang,⁹ E. Widmann,⁷⁶ H. Yamamoto,⁸³ S. B. Yang,³⁸ H. Ye,⁷ C. Z. Yuan,²⁶ Y. Yusa,⁶³ Z. P. Zhang,⁷¹ V. Zhilich,^{4,64} V. Zhukova,⁴² and V. Zhulanov^{4,64}

(The Belle Collaboration)

¹University of the Basque Country UPV/EHU, 48080 Bilbao

²Beihang University, Beijing 100191

³Brookhaven National Laboratory, Upton, New York 11973

⁴Budker Institute of Nuclear Physics SB RAS, Novosibirsk 630090

⁵Faculty of Mathematics and Physics, Charles University, 121 16 Prague

⁶University of Cincinnati, Cincinnati, Ohio 45221

⁷Deutsches Elektronen-Synchrotron, 22607 Hamburg

⁸University of Florida, Gainesville, Florida 32611

⁹Key Laboratory of Nuclear Physics and Ion-beam Application (MOE) and Institute of Modern Physics, Fudan University, Shanghai 200443

¹⁰Justus-Liebig-Universität Gießen, 35392 Gießen

¹¹Gifu University, Gifu 501-1193

¹²II. Physikalisches Institut, Georg-August-Universität Göttingen, 37073 Göttingen

¹³SOKENDAI (The Graduate University for Advanced Studies), Hayama 240-0193

¹⁴Gyeongsang National University, Chinju 660-701

¹⁵Hanyang University, Seoul 133-791

¹⁶University of Hawaii, Honolulu, Hawaii 96822

¹⁷High Energy Accelerator Research Organization (KEK), Tsukuba 305-0801

¹⁸J-PARC Branch, KEK Theory Center, High Energy Accelerator Research Organization (KEK), Tsukuba 305-0801

¹⁹Forschungszentrum Jülich, 52425 Jülich

²⁰IKERBASQUE, Basque Foundation for Science, 48013 Bilbao

²¹Indian Institute of Technology Bhubaneswar, Satya Nagar 751007

²²Indian Institute of Technology Guwahati, Assam 781039

²³Indian Institute of Technology Hyderabad, Telangana 502285

²⁴Indian Institute of Technology Madras, Chennai 600036

²⁵Indiana University, Bloomington, Indiana 47408

- ²⁶*Institute of High Energy Physics, Chinese Academy of Sciences, Beijing 100049*
- ²⁷*Institute of High Energy Physics, Vienna 1050*
- ²⁸*INFN—Sezione di Napoli, 80126 Napoli*
- ²⁹*INFN—Sezione di Torino, 10125 Torino*
- ³⁰*Advanced Science Research Center, Japan Atomic Energy Agency, Naka 319-1195*
- ³¹*J. Stefan Institute, 1000 Ljubljana*
- ³²*Institut für Experimentelle Teilchenphysik, Karlsruher Institut für Technologie, 76131 Karlsruhe*
- ³³*Kennesaw State University, Kennesaw, Georgia 30144*
- ³⁴*King Abdulaziz City for Science and Technology, Riyadh 11442*
- ³⁵*Department of Physics, Faculty of Science, King Abdulaziz University, Jeddah 21589*
- ³⁶*Kitasato University, Sagami 252-0373*
- ³⁷*Korea Institute of Science and Technology Information, Daejeon 305-806*
- ³⁸*Korea University, Seoul 136-713*
- ³⁹*Kyungpook National University, Daegu 702-701*
- ⁴⁰*LAL, University Paris-Sud, CNRS/IN2P3, Université Paris-Saclay, Orsay*
- ⁴¹*École Polytechnique Fédérale de Lausanne (EPFL), Lausanne 1015*
- ⁴²*P.N. Lebedev Physical Institute of the Russian Academy of Sciences, Moscow 119991*
- ⁴³*Faculty of Mathematics and Physics, University of Ljubljana, 1000 Ljubljana*
- ⁴⁴*Ludwig Maximilians University, 80539 Munich*
- ⁴⁵*Luther College, Decorah, Iowa 52101*
- ⁴⁶*Malaviya National Institute of Technology Jaipur, Jaipur 302017*
- ⁴⁷*University of Malaya, 50603 Kuala Lumpur*
- ⁴⁸*University of Maribor, 2000 Maribor*
- ⁴⁹*Max-Planck-Institut für Physik, 80805 München*
- ⁵⁰*School of Physics, University of Melbourne, Victoria 3010*
- ⁵¹*University of Mississippi, University, Mississippi 38677*
- ⁵²*University of Miyazaki, Miyazaki 889-2192*
- ⁵³*Moscow Physical Engineering Institute, Moscow 115409*
- ⁵⁴*Moscow Institute of Physics and Technology, Moscow Region 141700*
- ⁵⁵*Graduate School of Science, Nagoya University, Nagoya 464-8602*
- ⁵⁶*Kobayashi-Maskawa Institute, Nagoya University, Nagoya 464-8602*
- ⁵⁷*Università di Napoli Federico II, 80055 Napoli*
- ⁵⁸*Nara Women's University, Nara 630-8506*
- ⁵⁹*National Central University, Chung-li 32054*
- ⁶⁰*National United University, Miao Li 36003*
- ⁶¹*Department of Physics, National Taiwan University, Taipei 10617*
- ⁶²*H. Niewodniczanski Institute of Nuclear Physics, Krakow 31-342*
- ⁶³*Niigata University, Niigata 950-2181*
- ⁶⁴*Novosibirsk State University, Novosibirsk 630090*
- ⁶⁵*Osaka City University, Osaka 558-8585*
- ⁶⁶*Pacific Northwest National Laboratory, Richland, Washington 99352*
- ⁶⁷*Panjab University, Chandigarh 160014*
- ⁶⁸*Peking University, Beijing 100871*
- ⁶⁹*University of Pittsburgh, Pittsburgh, Pennsylvania 15260*
- ⁷⁰*Theoretical Research Division, Nishina Center, RIKEN, Saitama 351-0198*
- ⁷¹*University of Science and Technology of China, Hefei 230026*
- ⁷²*Seoul National University, Seoul 151-742*
- ⁷³*Showa Pharmaceutical University, Tokyo 194-8543*
- ⁷⁴*Soongsil University, Seoul 156-743*
- ⁷⁵*University of South Carolina, Columbia, South Carolina 29208*
- ⁷⁶*Stefan Meyer Institute for Subatomic Physics, Vienna 1090*
- ⁷⁷*Sungkyunkwan University, Suwon 440-746*
- ⁷⁸*School of Physics, University of Sydney, New South Wales 2006*
- ⁷⁹*Department of Physics, Faculty of Science, University of Tabuk, Tabuk 71451*
- ⁸⁰*Tata Institute of Fundamental Research, Mumbai 400005*
- ⁸¹*Department of Physics, Technische Universität München, 85748 Garching*
- ⁸²*Toho University, Funabashi 274-8510*
- ⁸³*Department of Physics, Tohoku University, Sendai 980-8578*
- ⁸⁴*Earthquake Research Institute, University of Tokyo, Tokyo 113-0032*
- ⁸⁵*Department of Physics, University of Tokyo, Tokyo 113-0033*

⁸⁶*Tokyo Institute of Technology, Tokyo 152-8550*⁸⁷*Tokyo Metropolitan University, Tokyo 192-0397*⁸⁸*Virginia Polytechnic Institute and State University, Blacksburg, Virginia 24061*⁸⁹*Wayne State University, Detroit, Michigan 48202*⁹⁰*Yamagata University, Yamagata 990-8560*⁹¹*Yonsei University, Seoul 120-749*

(Received 15 October 2018; published 29 January 2019)

We search for CP violation in the singly-Cabibbo-suppressed decay $D^0 \rightarrow K^+K^-\pi^+\pi^-$ using data corresponding to an integrated luminosity of 988 fb^{-1} collected by the Belle detector at the KEKB e^+e^- collider. We measure a set of five kinematically dependent CP asymmetries, of which four asymmetries are measured for the first time. The set of asymmetry measurements can be sensitive to CP violation via interference between the different partial-wave contributions to the decay and performed on other pseudoscalar decays. We find no evidence of CP violation.

DOI: [10.1103/PhysRevD.99.011104](https://doi.org/10.1103/PhysRevD.99.011104)

Charge-conjugation and parity (CP) symmetry violation has been observed in various weak decays involving strange and beauty quarks [1] and is well described in the standard model (SM) by the Cabibbo-Kobayashi-Maskawa matrix [2]. But the magnitude of CP violation in the SM is too small to explain the baryon asymmetry in the visible universe [3]. Therefore, the search for additional processes that violate CP symmetry, which are not described by the SM, is of great interest to explain the matter-dominant universe. CP violation in the charm sector is expected to be small, less than $\mathcal{O}(10^{-3})$ in the SM [4,5], which makes it an excellent probe for CP violation beyond that of the SM [1].

CP violation in the singly-Cabibbo-suppressed decay $D^0 \rightarrow K^+K^-\pi^+\pi^-$ was searched for using \hat{T} -odd correlations [6–8], where \hat{T} reverses the direction of momenta and spin, which is different from the usual time reversal operator T [9]. No CP violation is observed up to now, but the \hat{T} -odd correlation measured may be weakly sensitive to CP violation in this decay [9]. In this paper, we report the first measurement of a set of CP -violating kinematic asymmetries in $D^0 \rightarrow K^+K^-\pi^+\pi^-$ decays. The set of kinematic asymmetries probes the rich variety of interfering contributions in a decay, which can be sensitive to non-SM CP -violating phases.

Assuming CPT symmetry, we construct a CP -violating asymmetry by comparing amplitudes of the decay with their CP -conjugate amplitudes. Amplitudes of the decay can be extracted from \mathcal{A}_X , which we define as

$$\mathcal{A}_X \equiv \frac{\Gamma(X > 0) - \Gamma(X < 0)}{\Gamma(X > 0) + \Gamma(X < 0)}, \quad (1)$$

where X is a kinematic variable, such as the vector triple product of the final-state momenta used in Refs. [6–8], $\Gamma(X > 0)$ is the rate for D^0 decays in which $X > 0$; and $\Gamma(X < 0)$, for D^0 decays in which $X < 0$. The CP -conjugated amplitudes can be extracted similarly for \bar{D}^0 decays using \bar{X} . We can then define our CP -violating kinematic asymmetry as

$$a_X^{CP} \equiv \frac{1}{2}(\mathcal{A}_X - \eta_X^{CP}\bar{\mathcal{A}}_{\bar{X}}), \quad (2)$$

where η_X^{CP} is a CP eigenvalue specific to X .

We measure a set of kinematic asymmetries for five different X , where four asymmetries are measured for the first time and one asymmetry is proportional to the \hat{T} -odd correlation using the vector triple product of the final-state momenta, which has been measured previously [6–8]. The set can be sensitive to CP violation in the interference between the S -wave and P -wave production of the K^+K^- and $\pi^+\pi^-$ pairs in the $D^0 \rightarrow K^+K^-\pi^+\pi^-$ decay, where the process of a quasi-two-body decay to a dikaon system and dipion system contributes to over 40% of the decay rate [1]. It covers the asymmetries that can be measured without considering the mass of the intermediate particles. The kinematic variables are constructed from the angles θ_1 , θ_2 , and Φ , which are shown in Fig. 1. The θ_1 is the angle between the K^+ momentum and the direction opposite to that of the D^0 momentum in the center-of-mass (CM) frame of the K^+K^- system. The θ_2 is defined in the same way as θ_1 substituting K^+ with π^+ and K^+K^- with $\pi^+\pi^-$. The Φ is the angle between the decay planes of the K^+K^- and $\pi^+\pi^-$ pairs in the CM frame of D^0 . Three kinematic variables have $\eta_X^{CP} = -1$: $\sin 2\Phi$, $\cos \theta_1 \cos \theta_2 \sin \Phi$, and $\sin \Phi$; the last variable is proportional to the vector triple product of the final-state momenta. The remaining two kinematic

*Corresponding author.
eunil@hep.korea.ac.kr

Published by the American Physical Society under the terms of the Creative Commons Attribution 4.0 International license. Further distribution of this work must maintain attribution to the author(s) and the published article's title, journal citation, and DOI. Funded by SCOAP³.

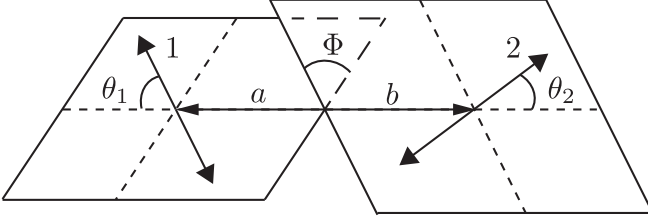


FIG. 1. Diagram showing the helicity angles θ_1 , θ_2 and Φ .

variables have $\eta_X^{CP} = +1$: $\cos \Phi$ and $\cos \theta_1 \cos \theta_2 \cos \Phi$. The kinematic asymmetries where η_X^{CP} is -1 , commonly known as \hat{T} -odd correlations, are dependent on the imaginary part of the interference of amplitudes for production of the K^+K^- and $\pi^+\pi^-$ states in different spin configurations [10–13]. The asymmetries where η_X^{CP} is $+1$, are dependent on the real part of the interference of amplitudes. Both types of asymmetries are nonzero in the case of CP violation. This set is measured for the first time for any four-body final state; these measurements can be performed for any other pseudoscalar meson that decays to four pseudoscalar mesons.

This analysis uses the data sample recorded by the Belle detector [14] at the e^+e^- asymmetric-energy collider KEKB [15], where the CM energy of the collisions was varied from the mass of the $Y(1S)$ resonance up to that of the $Y(6S)$ resonance. The total data sample corresponds to an integrated luminosity of 988 fb^{-1} [16].

Monte Carlo (MC) samples are used to devise the selection criteria, identify the different sources of background, model the data, validate the fit procedure, and determine systematic uncertainties. Inclusive MC samples were generated with EVTGEN [17], where the number of generated events corresponds to six times the integrated luminosity of the data sample. The detector response was simulated with GEANT3 [18]. To simulate the effect of beam-induced background, the generated events have data solely due to the beam backgrounds overlaid.

Since the final state is self-conjugate, the flavor of the D^0 mesons is identified by reconstructing the decay chains $D^{*+} \rightarrow D^0 \pi_s^+$, with D^0 decaying into $K^+K^-\pi^+\pi^-$, where π_s^+ is referred to as the slow pion. Here, and elsewhere in this paper, charge-conjugate states are implied unless stated explicitly otherwise.

Using MC simulated data, we developed the selection criteria to maximize a figure of merit of $S/\sqrt{S+B}$, where S is the signal yield and B is the background yield in a signal enhanced region, which is defined to be within $1.5 \text{ MeV}/c^2$ of the known D^0 mass [1] and within $0.25 \text{ MeV}/c^2$ of the known mass difference (Δm) between the D^{*+} candidate and its daughter D^0 [1].

We select charged tracks that originate from close to the e^+e^- interaction point (IP) by requiring the impact parameters to be less than 4 cm in the beam direction and 2 cm in the plane transverse to the beam direction. To ensure the

tracks are well reconstructed, we require they each have a transverse momentum greater than $0.1 \text{ GeV}/c$ and at least two associated hits in the silicon vertex detector in both the beam direction and azimuthal direction. Charged tracks are identified as pions or kaons depending on the ratio of particle identification likelihoods $\mathcal{L}_K/(\mathcal{L}_K + \mathcal{L}_\pi)$, which are constructed from information recorded by the central drift chamber, time-of-flight scintillation counters, and aerogel threshold Cherenkov counter. We identify a charged track as a kaon when this ratio is above 0.6; otherwise it is assumed to be a pion. The kaon and pion identification efficiencies are typically over 80%, and the misidentification probabilities are below 10% [19].

We form a D^0 candidate from each combination of two oppositely charged kaon tracks and two oppositely charged pion tracks. We require each D^0 candidate have an invariant mass within $30 \text{ MeV}/c^2$ of the known D^0 mass [1,20], where the range is larger than 7 times the mass resolution of the reconstructed D^0 candidate, and a momentum in the CM frame greater than $1.8 \text{ GeV}/c$. For each surviving candidate, we perform a vertex- and mass-constrained fit to the kaons and pions; we require the vertex fit to have a probability greater than 0.1%. We also perform a fit where each D^0 candidate is fit under the hypothesis that the trajectory of the candidate originates from the IP and require the fit to have a probability greater than 0.005%.

To veto the Cabibbo-favored $D^0 \rightarrow K^+K^-K_S^0$ decays, we remove D^0 candidates whose daughter pion pairs have invariant masses within $12.05 \text{ MeV}/c^2$ of the known K_S^0 mass [1], which is five times the mass resolution of the reconstructed K_S^0 candidate.

We form each combination of a positively charged pion track and D^0 candidate into a D^{*+} candidate and perform a vertex fit on the pion, where the fit is constrained to the intersection of the D^0 candidate trajectory with the IP region. We require each D^{*+} candidate have a momentum in the CM frame greater than $2.5 \text{ GeV}/c$. We also require Δm to be within ${}_{-5.9}^{+7.6} \text{ MeV}/c^2$ of the known Δm [1], where the lower limit corresponds to the known π^\pm mass.

In the signal region, 8.1% of events have multiple D^{*+} and/or D^{*-} candidates, while the average multiple candidates per event is 1.1, which is comparable with Ref. [21]. We select either a D^{*+} or D^{*-} candidate for each event, based on the smallest χ^2 for the D^0 mass fit. If there are multiple D^{*+} and/or D^{*-} candidates formed with this D^0 , we select the one whose π_s^+ or π_s^- has the smallest impact parameter in the transverse plane. Studies with the MC sample indicate that 93% of the multiple-candidate events are correctly selected. The efficiency for the $D^0 \rightarrow K^+K^-\pi^+\pi^-$ decay with the stated selections is 11%. A total of 474,971 events are reconstructed from the data sample.

After all selection criteria, our data sample contains events that fall into four different categories: correctly

reconstructed D^0 mesons coming from correctly reconstructed D^{*+} mesons, which we call signal events; events with correctly reconstructed D^0 mesons coming from misreconstructed D^{*+} candidates, which we call random- π_s events; events with a partially reconstructed D^0 candidate and the π_s^+ from a D^{*+} , which we call partial- D^* events, which has a small peak in the signal region of Δm ; and events with both D^0 and D^{*+} candidates misreconstructed, which we call combinatorial events. Our selection criteria rejects over 99% of events with $D_s^+ \rightarrow K^+ K^- \pi^+ \pi^+ \pi^-$, which could be confused for our signal, leaving a negligible number of such events.

We calculate the CP -violating kinematic asymmetry with the yield of the signal events for each flavor of D^0 and each sign of the relevant kinematic variable. To do this, we perform four separate fits to the data for each kinematic variable. Each fit is a binned two-dimensional extended maximum-likelihood fit to the reconstructed D^0 mass and Δm . The data are binned into 200 equal-width bins in each dimension. These additional requirements on $m(K^+ K^- \pi^+ \pi^-)$ and Δm have a negligible effect on the selection efficiency.

One model is used for all fits. It contains components describing signal, random π_s , partial- D^* , and combinatorial events. The yield of each component is free in each fit, but parameters governing the shapes of the components are fixed from a single fit to all the data regardless of D^0 flavor and X .

The signal component is the product of a sum of bifurcated Gaussian and Gaussian probability density functions (PDFs) for $m(K^+ K^- \pi^+ \pi^-)$ and a sum of Gaussian and JohnsonSU [22] PDFs for Δm . The combinatorial component is the product of a Chebyshev function for $m(K^+ K^- \pi^+ \pi^-)$ and a threshold function for Δm . The random- π_s component is the product of the signal shape for $m(K^+ K^- \pi^+ \pi^-)$ and the combinatorial shape for Δm . And the partial- D^* component is the product of a Chebyshev function for $m(K^+ K^- \pi^+ \pi^-)$ and a Bifurcated Gaussian PDF for Δm , where the shape parameters for the partial- D^* component are fixed to those obtained from a fit to an inclusive MC sample. The shape of the MC sample is validated by comparing it to data in the sidebands of the $m(K^+ K^- \pi^+ \pi^-)$ distribution; the shapes are compatible.

Figure 2 shows the results of the fit to all the data, from which the shapes of all components are fixed for all remaining fits; the model agrees well with the data, as can be seen from the pulls, which are defined as the difference between the data points and the model expectation divided by the expected uncertainty. As an example of a set of fits used to determine the CP -violating kinematic asymmetry, we show separate fit results for positive and negative $\sin 2\Phi$ for D^0 samples in Fig. 3. The signal yields determined by the fits are given in Table I for each D^0 flavor and kinematic variable sign.

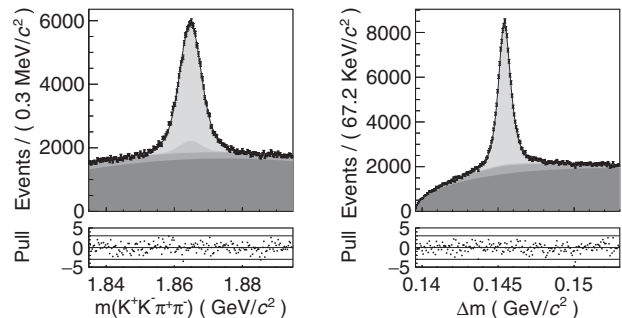


FIG. 2. Data (black points) and fit results (shaded regions) for the fit to all the data in projections of $m(K^+ K^- \pi^+ \pi^-)$ (left) and Δm (right). The shaded regions are stacked upon each other and show, from lowest to highest, the combinatorial, partial- D^* , random- π_s , and signal components. The lower plots show the pulls for the fit; the unlabeled horizontal lines indicate ± 3 .

We perform several cross checks to validate our analysis: To study the effect of the $D^0 \rightarrow K^* \bar{K}^*$, where K^* decays to $K^+ \pi^-$, we recalculate the asymmetries including a veto on K^* and \bar{K}^* that rejects the D^0 candidates with a $K^+ \pi^-$ pair and $K^- \pi^+$ pair of an invariant mass within $80 \text{ MeV}/c^2$ of the known K^* mass [1], which is twenty times the mass resolution of the reconstructed K^* candidate. The recalculated asymmetries are consistent with the values without the veto.

To study the effects from the best candidate selection, we recalculate the asymmetries with no best candidate

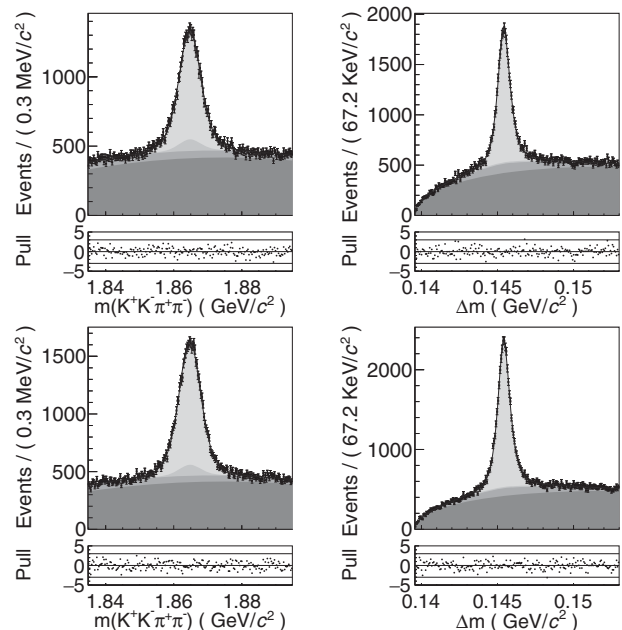


FIG. 3. Two-dimensional fit results, distributions and pull of the data subsamples projected on the observables $m(K^+ K^- \pi^+ \pi^-)$ (left) and Δm (right). The distribution sequence follows Fig. 2. Top histograms show the $D^0(\sin 2\Phi > 0)$ subsample while the bottom histograms show the $D^0(\sin 2\Phi < 0)$ subsample.

TABLE I. Fit results for the yield of signal in the subsamples of each kinematic variable X . The uncertainties are statistical only.

X	$D^0(X > 0)$	$D^0(X < 0)$	$\bar{D}^0(\bar{X} > 0)$	$\bar{D}^0(\bar{X} < 0)$
$\cos \Phi$	$21, 913 \pm 181$	$32, 544 \pm 216$	$21, 657 \pm 180$	$32, 623 \pm 216$
$\sin \Phi$	$29, 177 \pm 205$	$25, 277 \pm 194$	$25, 474 \pm 194$	$28, 800 \pm 204$
$\sin 2\Phi$	$23, 096 \pm 187$	$31, 355 \pm 211$	$31, 455 \pm 211$	$22, 805 \pm 186$
$\cos \theta_1 \cos \theta_2 \cos \Phi$	$31, 065 \pm 211$	$23, 398 \pm 188$	$30, 963 \pm 210$	$23, 304 \pm 187$
$\cos \theta_1 \cos \theta_2 \sin \Phi$	$26, 016 \pm 196$	$28, 441 \pm 203$	$28, 353 \pm 203$	$25, 919 \pm 195$

selection. The recalculated asymmetries are consistent with those calculated including the best candidate selection.

The detector resolution of the kinematic variables could affect the asymmetries. We measure the fraction of cross-feed between signal events with $X > 0$ and $X < 0$ using an MC sample that has a similar shape to the data. The fraction of cross-feed is at the 1% level, making its effect negligible.

We estimate the effect of incorrectly assigning the flavor of the D^0 using an MC sample that has a similar integrated luminosity to the data. In the MC sample, incorrectly assigned events comprise less than 0.01% of the total number of events. Misassignment has a negligible effect.

There could be an effect due to an efficiency difference depending on the kinematic variable regions. Efficiencies depending on kinematic variable regions are measured using a MC sample. We find that the efficiency does not depend on the kinematic variables used to define the asymmetries.

Several sources of systematic uncertainty are considered. Individual uncertainties and the total systematic uncertainty are listed in Table II. The bias from the model PDF is estimated by changing the signal model, partial- D^* model, and combinatorial model. We change the signal model and partial- D^* model to products of one-dimensional Gaussian-kernel-estimated PDFs [23] and the combinatorial model to a product of one-dimensional PDFs obtained from an inclusive MC sample. The difference between the measured values is assigned as a systematic uncertainty.

The detector bias is estimated from a control sample of $D^0 \rightarrow K^- \pi_{\text{low}}^+ \pi^- \pi_{\text{high}}^+$ events, where momentum is used to differentiate between the π_{high}^+ and π_{low}^+ . This decay is Cabibbo-favored in which all kinematic asymmetries are expected to be much smaller than the measurement

precision [4]. The kinematic variables are calculated in the same way as for the $K^+ K^- \pi^+ \pi^-$ final state, substituting K^+ with π_{low}^+ . The kinematic asymmetries are found to be consistent with zero, and we assign their statistical uncertainties as the systematic uncertainties related to any detector bias.

To assess whether there is a bias introduced by the likelihood fit and to check the extraction of kinematic asymmetries from the two-dimensional binned fit, we generate MC samples with different asymmetries and compare the fit results with the generated values. The average difference between the measured and generated value is assigned as a systematic uncertainty.

The various sources of systematic uncertainty are independent of each other. Therefore we estimate the total systematic uncertainty by summing the uncertainties in quadrature. As a note, the kinematic asymmetries are constructed such that they are insensitive to the intrinsic production asymmetry [8].

The measured \mathcal{A}_X and $\bar{\mathcal{A}}_X$ are listed in Table III with statistical errors. As in other experiments [7,8], final state interaction effects are observed with a similar amplitude for $\mathcal{A}_{\sin \Phi}$ and $\bar{\mathcal{A}}_{\sin \Phi}$. We find the CP -violating kinematic asymmetries to be

$$a_{\cos \Phi}^{CP} = (3.4 \pm 3.6 \pm 0.6) \times 10^{-3}, \quad (3)$$

$$a_{\sin \Phi}^{CP} = (5.2 \pm 3.7 \pm 0.7) \times 10^{-3}, \quad (4)$$

$$a_{\sin 2\Phi}^{CP} = (3.9 \pm 3.6 \pm 0.7) \times 10^{-3}, \quad (5)$$

$$a_{\cos \theta_1 \cos \theta_2 \cos \Phi}^{CP} = (-0.2 \pm 3.6 \pm 0.7) \times 10^{-3}, \quad (6)$$

TABLE II. Contributions to the systematic uncertainty (in per mille) for each CP -violating kinematic asymmetry a_X^{CP} .

Effect	$a_{\cos \Phi}^{CP}$	$a_{\sin \Phi}^{CP}$	$a_{\sin 2\Phi}^{CP}$	$a_{\cos \theta_1 \cos \theta_2 \cos \Phi}^{CP}$	$a_{\cos \theta_1 \cos \theta_2 \sin \Phi}^{CP}$
Signal model PDF	0.1	0.3	0.1	0.2	0.0
Partial- D^* model PDF	0.1	0.1	0.2	0.2	0.0
Combinatorial model PDF	0.1	0.1	0.3	0.0	0.3
Detector bias	0.6	0.6	0.6	0.6	0.6
Likelihood fit bias	0.1	0.1	0.1	0.1	0.1
Total	0.6	0.7	0.7	0.7	0.7

TABLE III. \mathcal{A}_X and $\bar{\mathcal{A}}_X$ (in per mille) for each kinematic variable X . The uncertainties are statistical only.

X	\mathcal{A}_X	$\bar{\mathcal{A}}_X$
$\cos \Phi$	-195.2 ± 5.1	202.0 ± 5.1
$\sin \Phi$	71.6 ± 5.2	61.3 ± 5.2
$\sin 2\Phi$	-151.7 ± 5.2	-159.4 ± 5.1
$\cos \theta_1 \cos \theta_2 \cos \Phi$	140.8 ± 5.1	-141.2 ± 5.2
$\cos \theta_1 \cos \theta_2 \sin \Phi$	-44.5 ± 5.2	-44.9 ± 5.2

$$a_{\cos \theta_1 \cos \theta_2 \sin \Phi}^{CP} = (0.2 \pm 3.7 \pm 0.7) \times 10^{-3}, \quad (7)$$

where the first and second uncertainties are statistical and systematic, respectively. These results indicate that there is no CP violation within the statistical and systematic uncertainties for the interferences between the S-wave and P-wave production of the K^+K^- and $\pi^+\pi^-$ pairs in this decay. No effects from new physics models can be observed within the experimental uncertainties. With more data from future experiments, it may be possible to measure the CP violation due to the SM in this decay.

In conclusion, we search for CP violation in $D^0 \rightarrow K^+K^-\pi^+\pi^-$ by measuring a set of five kinematic asymmetries. The set of measurements can be sensitive

to CP violation via the rich variety of interference between the different partial-wave contributions to the decay. It can be performed on any other pseudoscalar meson that decays into four pseudoscalar mesons. Four asymmetries are measured for the first time. The set of CP -violating kinematic asymmetries is consistent with CP conservation and provide new constraints on new physics models [4,9,11].

We thank the KEKB group for excellent operation of the accelerator; the KEK cryogenics group for efficient solenoid operations; and the KEK computer group, the NII, and PNNL/EMSL for valuable computing and SINET5 network support. We acknowledge support from MEXT, JSPS and Nagoya's TLPRC (Japan); ARC (Australia); FWF (Austria); NSFC and CCEPP (China); MSMT (Czechia); CZF, DFG, EXC153, and VS (Germany); DST (India); INFN (Italy); MOE, MSIP, NRF, RSRI, FLRFAS project and GSDC of KISTI and KREONET/GLORIAD (Korea); MNiSW and NCN (Poland); MSHE, Grant No. 14.W03.31.0026 (Russia); ARRS (Slovenia); IKERBASQUE and MINECO (Spain); SNSF (Switzerland); MOE and MOST (Taiwan); and DOE and NSF (USA). E. W. is partially supported by NRF-2017R1A2B3001968.

-
- [1] M. Tanabashi *et al.* (Particle Data Group), *Phys. Rev. D* **98**, 030001 (2018).
- [2] M. Kobayashi and T. Maskawa, *Prog. Theor. Phys.* **49**, 652 (1973).
- [3] M. Trodden, *Rev. Mod. Phys.* **71**, 1463 (1999).
- [4] Y. Grossman, A. L. Kagan, and Y. Nir, *Phys. Rev. D* **75**, 036008 (2007).
- [5] J. Brod, A. L. Kagan, and J. Zupan, *Phys. Rev. D* **86**, 014023 (2012).
- [6] J. Link *et al.* (FOCUS Collaboration), *Phys. Lett. B* **622**, 239 (2005).
- [7] P. del Amo Sanchez *et al.* (BABAR Collaboration), *Phys. Rev. D* **81**, 111103 (2010).
- [8] R. Aaij *et al.* (LHCb Collaboration), *J. High Energy Phys.* **10** (2014) 005.
- [9] G. Durieux and Y. Grossman, *Phys. Rev. D* **92**, 076013 (2015).
- [10] M. Gronau and J. L. Rosner, *Phys. Rev. D* **84**, 096013 (2011).
- [11] B. Bhattacharya, A. Datta, M. Duraisamy, and D. London, *Phys. Rev. D* **88**, 016007 (2013).
- [12] R. Aaij *et al.* (LHCb Collaboration), *J. High Energy Phys.* **07** (2015) 166.
- [13] J. Koerner and G. R. Goldstein, *Phys. Lett.* **89B**, 105 (1979).
- [14] A. Abashian *et al.* (Belle Collaboration), *Nucl. Instrum. Methods Phys. Res., Sect. A* **479**, 117 (2002); also see detector section in J. Brodzicka *et al.*, *Prog. Theor. Exp. Phys.* **2012**, 04D001 (2012).
- [15] S. Kurokawa and E. Kikutani, *Nucl. Instrum. Methods Phys. Res., Sect. A* **499**, 1 (2003), and other papers included in this Volume; T. Abe *et al.*, *Prog. Theor. Exp. Phys.* **2013**, 03A001 and references therein.
- [16] J. Brodzicka *et al.* (Belle Collaboration), *Prog. Theor. Exp. Phys.* **2012**, 04D001 (2012).
- [17] D. J. Lange, *Nucl. Instrum. Methods Phys. Res., Sect. A* **462**, 152 (2001).
- [18] R. Brun, F. Bruyant, M. Maire, A. C. McPherson, and P. Zanarini, Report No. CERN-DD-EE-84-1, 1987.
- [19] E. Nakano, *Nucl. Instrum. Methods Phys. Res., Sect. A* **494**, 402 (2002).
- [20] A. Tomaradze, S. Dobbs, T. Xiao, K. K. Seth, and G. Bonvicini, *Phys. Rev. D* **89**, 031501 (2014).
- [21] E. White *et al.* (Belle Collaboration), *Phys. Rev. D* **88**, 051101 (2013).
- [22] N. L. Johnson, *Biometrika* **36**, 149 (1949).
- [23] K. Cranmer, *Comput. Phys. Commun.* **136**, 198 (2001).